Polymer Journal (2010) 42, 386–390

www.nature.com/pj

ORIGINAL ARTICLE

Second and third virial coefficients of low-molecular-weight polystyrene with a benzyl end in toluene

Hiroshi Okada, Shuhei Matsumoto and Yo Nakamura

Light-scattering measurements were taken on six samples of polystyrene (PS) with a benzyl group at one end of the chain (benzyl-PS) in toluene at 15 °C. The second and third virial coefficients (A_2 and A_3, respectively) were determined as functions of weight-average molecular weight, M_w, which ranges from 6.0×10^2 to 1.2×10^4. It was found that values of A_2 for benzyl-PS were systematically smaller than those for PS with a butyl group at one end of the chain (butyl-PS) and that the difference becomes larger with decreasing M_w. From the A_2 data obtained, the excess binary-cluster integral between the butyl end and the middle segments was estimated to be about three times larger than the binary-cluster integral between the benzyl end and the middle segments, where 'excess' means the difference from the binary-cluster integral between middle segments. The A_3 values for benzyl-PS for $M_w<10^4$ were also smaller than those for butyl-PS. If we assume a term independent of molecular weight in A_3, the excess ternary-cluster integral among one butyl end and two middle segments was estimated to be about five times larger than that among one benzyl end and two middle segments.
Polymer Journal (2010) **42,** 386–390; doi:10.1038/pj.2010.11; published online 10 March 2010

Keywords: chain-end effect; good solvent; light scattering; polystyrene; second virial coefficient; third virial coefficient

INTRODUCTION

Solution properties of long flexible polymers are discussed on the basis of the two-parameter theory.[1,2] However, this theory cannot describe properties in low-molecular-weight regions, in which effects from stiffness and/or local conformations of the chain, chain-end groups and three-segment interactions become essential.[3]

The importance of the effects of chain stiffness on A_2 was discussed by Yamakawa.[4] Einaga *et al.*[5] later showed that the effects of chain ends, as well as chain stiffness, must be considered to obtain a quantitative agreement between the theoretical and observed values of A_2 for polystyrene (PS) in toluene (a good solvent) for $M_w<10^4$, where M_w denotes the weight-average molecular weight. The PS samples used by Einaga *et al.*[5] had a butyl group at one end of the chain. If we perform a similar study on PS samples with different chain ends, different results may be obtained.

It is known that data for A_2 in cyclohexane solutions of PS with a butyl group (butyl-PS) versus PS with a benzyl group (benzyl-PS) at one end of the chain show very different tendencies for $M_w<10^4$ at the theta point (34.5 °C), where A_2 for sufficiently large M_w vanishes. The positive A_2 of butyl-PS increasing with decreasing M_w is attributed to effects from the chain ends.[4] On the other hand, values of A_2 for benzyl-PS became negative and decreased with decreasing M_w.[6] It was considered that the negative values of A_2 occurred because of the effects of the three-segment interactions and that effects from chain ends were negligibly small. From these results on the theta solvent system, we may expect to reduce the chain-end effect on A_2 for a good solvent system by changing the chain end from a butyl group to a benzyl group.

Compared with A_2, the number of studies on the third virial coefficient, A_3, of polymer solutions is much smaller because of the difficulty of obtaining precise values. Sato *et al.*[7] overcame this problem by applying the Bawn plot[8] (see Results and Discussion section), which enables a separate determination of A_2 and A_3. Nakamura *et al.*[9] applied this plot to PS+benzene solutions to obtain systematic data on A_2 and A_3 as functions of M_w. They showed that the reduced third virial coefficient, g, defined by $A_3/A_2^2M_w$, is an increasing function of M_w for $M_w\gtrsim10^5$. This is consistent with the prediction from the two-parameter theory, except that the values of g were almost constant for $10^4\lesssim M_w\lesssim10^5$. Norisuye *et al.*[10] examined g in the low-molecular-weight range and found that three-segment interaction has a more important role than chain stiffness. Later, Osa *et al.*[11] reached essentially the same conclusion from a study on poly (α-methylstyrene) in toluene. In these studies, only data for $M_w>10^4$ were discussed without considering the effects from chain ends. Because the effect of the chain end on A_3 of butyl-PS in cyclohexane is known to be remarkable for $M_w\lesssim10^4$,[12] the same effect on A_3 should be considered for good solvent systems.

In this study, we performed light-scattering measurements to determine A_2 and A_3 for benzyl-PS, with M_w ranging from 6.0×10^2 to 1.2×10^4 in toluene at 15 °C. This enabled us to study the effects from the chain end and chain stiffness by comparing the results with the data for butyl-PS.[5]

Department of Polymer Chemistry, Kyoto University, Katsura, Kyoto, Japan
Correspondence: Dr Y Nakamura, Department of Polymer Chemistry, Kyoto University, Katsura, Kyoto 615-8510, Japan.
E-mail: yonaka@molsci.polym.kyoto-u.ac.jp
Received 1 December 2009; revised 14 January 2010; accepted 15 January 2010; published online 10 March 2010

EXPERIMENTAL PROCEDURE

Benzyl-PS samples (PS600, PS700, PS4800, PS8300 and PS12000) were obtained by anionic polymerization of styrene with benzyllithium as the initiator[13] in an argon atmosphere. These samples, except the two lowest molecular-weight samples, were fractionally precipitated with benzene as the solvent and methanol as the precipitant. Sample PS1900 was prepared in the previous study.[6] The number-average to weight-average molecular weight ratio, M_w/M_n, was determined by gel-permeation chromatography. Values were less than 1.06, as shown in Table 1. The two samples, PS600 and PS700, were obtained by fractionation of low-molecular-weight benzyl-PS by gel-permeation chromatography with chloroform as the eluent, and they were then reprecipitated from acetone solutions to water. These liquid samples were dried at 50 °C in a rotary evaporator for 2 weeks. Existence of the benzyl chain end was confirmed by ^{1}H-NMR and MALDI-TOF mass spectroscopy.

Each test solution was optically clarified by filtration through a double layer of Teflon filters, with 0.1 μm pores, into a cylindrical light-scattering cell. The cell had been rinsed with refluxing acetone for more than 1.5 h and dried overnight in a desiccator.

The polymer mass concentration, c, of each solution was calculated from the gravimetrically determined polymer weight fraction, w, multiplied by the solution density ρ, which was calculated from $\rho=\rho_0[1+(1-\bar{\nu}\rho_0)w]$. Here, ρ_0 and $\bar{\nu}$ denote the solvent density and the specific volume of the solute, respectively. The specific volumes for PS600 and PS700 were determined from density measurements of the solvent and the solutions by an Anton–Paar densitometer, DMA-5000 (Anton–Paar, Graz, Austria), as shown in Table 1. The value for the other samples was assumed to be 0.91 cm^3 g^{-1}.[14]

Light-scattering measurements were taken on a Fica 50 light-scattering photometer (Fica, Saint Denis, France) with vertically polarized light with a wavelength of 436 nm in an angular range from 22.5 to 142.5° to obtain the excess Rayleigh ratio, R_θ, at the scattering angle θ. The data for each solution were extrapolated to $\theta=0$ by plotting Kc/R_θ against $\sin^2\theta$ to obtain the zero-angle value Kc/R_0, where K represents the optical constant. Corrections of optical anisotropy were made for both solutions and solvent according to the following equation:

$$R_0 = (1-\tfrac{7}{6}\rho_u)R_0^*$$

Here, R_0* denotes the uncorrected R_0 and ρ_u is the depolarized ratio, which was determined by the method of Rubingh and Yu.[15]

The specific reflective index increments, $\partial n/\partial c$, measured by a modified Schulz—Cantow-type differential refractometer, are summarized in the fifth column of Table 1.

RESULTS AND DISCUSSION

Data analysis

The scattering intensities, extrapolated to $\theta=0$, were obtained as a function of c, for each polymer sample. Except PS600 and PS700, they were analyzed using the Bawn plot,[8] that is, $S(c_1,c_2)$, as defined by the following equation plotted against c_1+c_2:[7]

$$S(c_1, c_2) \equiv \frac{(Kc/R_0)_{c=c_2} - (Kc/R_0)_{c=c_1}}{c_2 - c_1} = 2A_2+3A_3(c_1+c_2)+\cdots \quad (1)$$

Here, $(Kc/R_0)_{c=c_i}$ means (Kc/R_0) at $c=c_i$ (i=1, 2). Figure 1 shows the Bawn plots for the samples indicated. Each plot can be fitted to a straight line. The slope and intercept at $c_1+c_2=0$ are equated to $3A_3$ and $2A_2$, respectively, according to Equation (1). We tried to apply the same plot to the data for PS600 and PS700, but we could not draw a line uniquely for each plot because of the considerable scattering of data points. For these samples, we applied the Berry plot,[16] that is, $(Kc/R_0)^{1/2}$ against c, as is shown in Figure 2. The slope and the intercept at $c=0$ of the fitted straight line for each plot are equated to $M_w^{1/2}A_2$ and $M_w^{-1/2}$, respectively. The values for A_2 and A_3, along with M_w, are summarized in Table 1.

Second virial coefficient

The dependence of A_2 on molecular weight is illustrated in Figure 3. The unfilled and filled circles represent the data points of A_2 for benzyl- and butyl-PS,[5] respectively, in toluene at 15 °C. The data points for benzyl-PS are systematically lower than those for butyl-PS. The difference becomes larger with decreasing M_w.

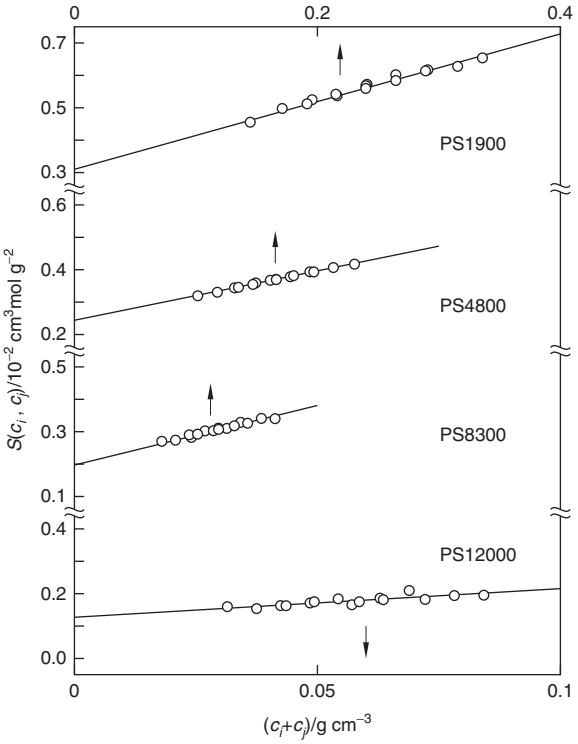

Figure 1 Bawn plots for benzyl-end polystyrene samples in toluene at 15 °C.

Table 1 Properties of benzyl-end polystyrene samples in toluene at 15 °C

Sample	$10^{-2}M_w$	M_w/M_n	$\bar{\nu}$ (cm^{3}g^{-1})	$\partial n/\partial c$ (cm^{3}g^{-1})	10^4A_2 (cm^{3}mol g^{-2})	10^3A_3 (cm^{6}mol g^{-3})
PS600	6.25	1.02	0.939	0.099_2	$25._0$	—
PS700	6.94	1.02	0.935	0.102_3	$21._6$	—
PS1900	19.8	1.06	—	0.106_0	$15._5$	3.5
PS4800	47.9	1.05	—	0.108_0	$12._2$	2.5
PS8300	83.2	1.04	—	0.109_8	9.8_5	2.9
PS12000	116	1.03	—	0.110_3	8.8_6	3.0

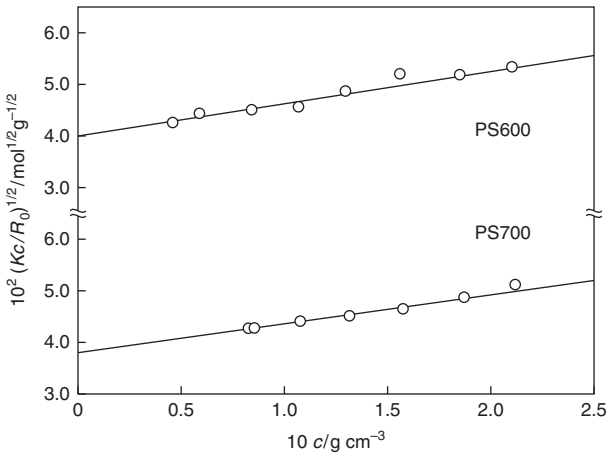

Figure 2 Square-root plots for benzyl-end polystyrene samples in toluene at 15 °C.

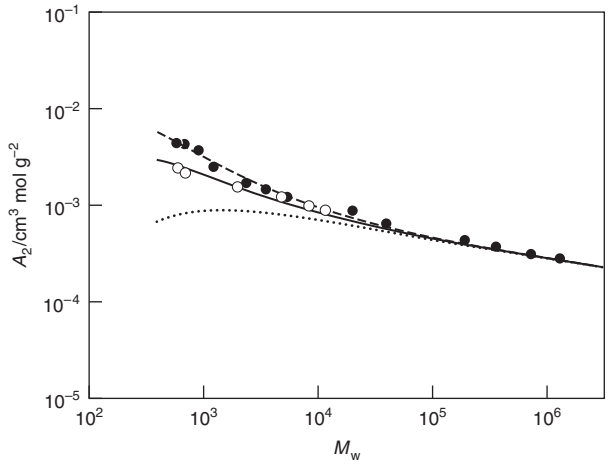

Figure 3 Dependence of A_2 on molecular weight for polystyrenes in toluene at 15.0 °C. Filled and unfilled circles represent data for butyl-end[5] and benzyl-end polystyrenes, respectively. The dotted curve indicates theoretical values without chain-end effects. Solid and dashed curves represent theoretical values with chain-end effects.

Theoretically, A_2 is expressed by the following equation:[4]

$$A_2 = A_2^{(\mathrm{HW})} + A_2^{(\mathrm{E})} \tag{2}$$

$A_2^{(\mathrm{HW})}$ represents the term for the binary interactions between chain segments, not including the contribution of the chain-end effects, and may be calculated from the following equation for the helical wormlike (HW) chain[3] with beads or segments arrayed along the chain contour with a distance of a:

$$A_2^{(\mathrm{HW})} = \frac{N_A c_\infty^{3/2} L^2 B}{2M^2} h \tag{3}$$

N_A, L and M denote the Avogadro constant, the contour length and molecular weight, respectively. c_∞ is expressed as[3]

$$c_\infty = \frac{4+(\lambda^{-1}\tau_0)^2}{4+(\lambda^{-1}\kappa_0)^2+(\lambda^{-1}\tau_0)^2} \tag{4}$$

with the stiffness parameter, λ^{-1}, and the differential geometrical curvature, κ_0, and torsion, τ_0. The excluded-volume parameter, B, is defined by

$$B = \frac{\beta_2}{a^2 c_\infty^{3/2}} \tag{5}$$

β_2 is the binary-cluster integral between *middle* segments. Here, the word *middle* means the segments excluding the ones at the chain ends. The dimensionless h in Equation (3) may be calculated from the modified Barrett equation[4,17] as a function of λB and λL with the scaled excluded-volume parameter (see Einaga *et al.*[5]).

The chain-end term, $A_2^{(\mathrm{E})}$, may be expressed as[4]

$$A_2^{(\mathrm{E})} = a_{2,1}M^{-1} + a_{2,2}M^{-2} \tag{6}$$

The constants $a_{2,1}$ and $a_{2,2}$ are defined as[4]

$$a_{2,1} = 2N_A\beta_{2,1}/M_0 \tag{7}$$

$$a_{2,2} = 2N_A\Delta\beta_{2,2} \tag{8}$$

with

$$\beta_{2,1} = (\beta_{01}+\beta_{02})/2 \tag{9}$$

$$\Delta\beta_{2,2} = (\beta_{11}+2\beta_{12}+\beta_{22})/4 - 2\beta_{2,1} \tag{10}$$

M_0 is the molecular weight for one segment. β_{ij} is the *excess* binary-cluster integral between segments i and j over the binary-cluster integral between the middle segments, β_2, where the subscripts 0, 1 and 2 represent the segments at the middle, at one of the chain ends and at the other chain end, respectively. A monomer unit is regarded as a segment.

The dotted line in Figure 3 represents the calculated $A_2^{(\mathrm{HW})}$ from Equation (3), with the following parameter set for PS in toluene:[18] M_L=358 nm^{-1}, λ^{-1}=2.06 nm, $\lambda^{-1}\kappa_0$=3.0, $\lambda^{-1}\tau_0$=6.0 and λB=0.33. M_L is the molecular weight for the unit contour length. The calculated values for $M_w \lesssim 10^5$ are systematically lower than both experimental values for butyl- and benzyl-PS. The difference between theoretical and experimental values becomes larger with decreasing M_w. By adding $A_2^{(\mathrm{E})}$ with $a_{2,1}$=2.5 cm^3 g^{-1} and $a_{2,2}$=−200 cm^3 mol^{-1},[5] we obtain the dashed line, which closely fits the experimental data for butyl-PS. The solid line calculated with $a_{2,1}$=1.4 cm^3 g^{-1} and $a_{2,2}$=−200 cm^3 mol^{-1} also closely fits the data for benzyl-PS. From Equation (7), with these values of $a_{2,1}$, we calculate $\beta_{2,1}$ for butyl- and benzyl-PS to be 0.22 and 0.12 nm^3, respectively.

Both ends of the benzyl-PS chain have the same chemical structure, because a polystyryl anion gives the benzyl structure when it is deactivated with a proton. Thus, we may regard $\beta_{01}=\beta_{02}$ in Equation (9) for benzyl-PS to obtain β_{01}=0.12 nm^3 for the binary interaction between the benzyl end and middle (or PS) segments. The structure of the terminated end of butyl-PS is the same as that of benzyl-PS. As the values for β_{01} for both polymers are the same, we obtain 0.32 nm^3 for β_{02} from Equation (9) with the above β_{01} and $\beta_{2,1}$ for butyl-PS. The value of β_{02}, which represents the binary interaction between the butyl end and middle segments, is about three times larger than β_{01} for the benzyl end.

Positive β_{01} shows that the *net* binary-cluster integral between the benzyl end and middle segments is larger than the one between *middle* segments, β_2. These results are rather different from those for PS in cyclohexane (34.5°C), a theta solvent, in which β_{01} is vanishingly small.[6] In this solvent, the binary-cluster integral between the benzyl end and middle (PS) segments may be incidentally close to the one between middle segments.

Third virial coefficient

Figure 4 shows the dependence of A_3 on molecular weight, in which literature data for butyl-PS in toluene at 15 °C[19] and those

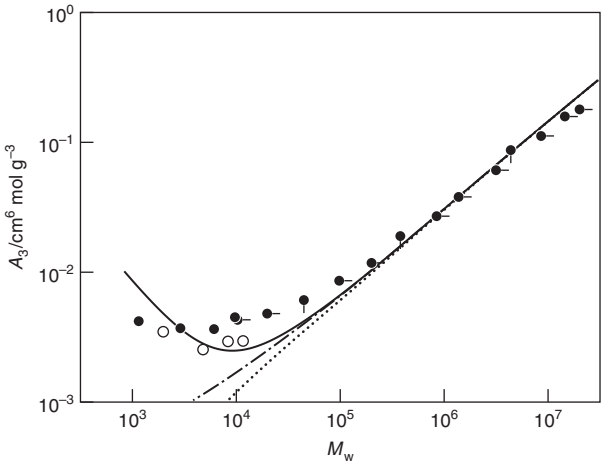

Figure 4 Dependence of A_3 on molecular weight for polystyrenes in good solvents. Filled and unfilled circles represent data for butyl-end (no pip, in toluene at 15 °C;[19] pip down[7] and right,[9] in benzene at 25 °C) and benzyl-end polystyrenes, respectively. Dotted, dot-dashed and solid curves represent theoretical values for $A_{3,\beta_2}^{(HW)}$, $A_{3,\beta_2}^{(HW)}+A_{3,\beta_3}^{(0)}$, and $A_{3,\beta_2}^{(HW)}+A_{3,\beta_3}^{(O)}+A_{3,\beta_3}^{(E)}$, respectively (with $\beta_3=4.7\times10^{-3}$ nm^6).

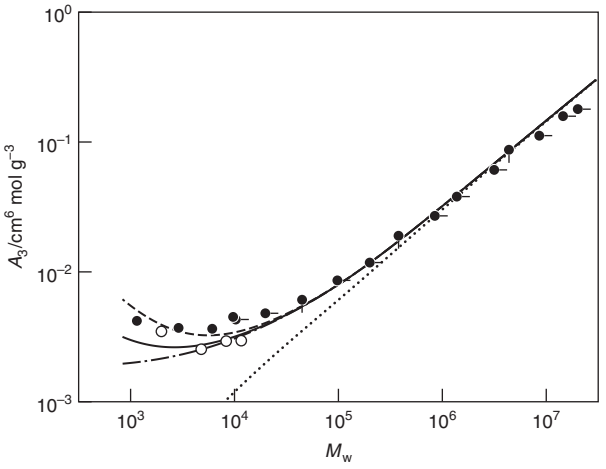

Figure 5 Dependence of A_3 on molecular weight for polystyrenes in good solvents. Symbols and dotted and dashed curves have the same meaning as those in Figure 4. Solid and dashed lines represent theoretical values for benzyl- and butyl-end polystyrenes, respectively (with $\beta_3=1.8\times10^{-2}$ nm^6).

for butyl-PS in benzene at 25 °C[7,9] are included. The values of A_3 for benzyl-PS from this study are slightly lower than those for butyl-PS.

The third virial coefficient for the linear chain may be expressed as[12]

$$A_3 = A_{3,\beta_2}^{(HW)}+A_{3,\beta_3} \tag{11}$$

The first and second terms on the right-hand side of the above equation correspond to the contribution of the binary- and ternary-segment interactions, respectively. We note that the remaining part, which includes cross terms of β_2 and β_3,[20] is ignored here because it is anticipated to be negligibly small.

The first term on the right-hand side of Equation (11) may be expressed as

$$A_{3,\beta_2}^{(HW)} = g_2[A_2^{(HW)}]^2M \tag{12}$$

g_2 may be calculated from the following equation:[10,11]

$$g_2 = 2.219\bar{z}(1+18\bar{z}+12.6\bar{z}^2)^{-1/2} \tag{13}$$

$\bar{z}$ is defined as

$$\bar{z} = \frac{z}{\alpha_S^3} \tag{14}$$

with

$$z = \left(\frac{3}{2\pi}\right)^{3/2}(\lambda B)(\lambda L)^{1/2} \tag{15}$$

The radius expansion factor, α_S, may be calculated from the modified Domb–Barrett equation:[21]

$$\alpha_S^2 = [1+10\tilde{z}+(70\pi/9+10/3)\tilde{z}^2+8\pi^{3/2}\tilde{z}^3]^{2/15} \times[0.933+0.067\exp(-0.85\tilde{z}-1.39\tilde{z}^2)] \tag{16}$$

with

$$\tilde{z} = \tfrac{3}{4}K(\lambda L)z \tag{17}$$

where $K(\lambda L)$ is a known function.[3,22]

The second term on the right-hand side of Equation (11) may be expressed as[12]

$$A_{3,\beta_3} = A_{3,\beta_3}^{(0)}+A_{3,\beta_3}^{(E)} \tag{18}$$

where the first term on the right-hand side represents the contribution from the interaction among three middle segments. The other term is for the interaction among two middle segments and one chain-end segment.

The zeroth-order contribution to the former term can be expressed as[1,23]

$$A_{3,\beta_3}^{(0)} = \frac{N_A^2n^3\beta_3}{3M^3} \tag{19}$$

with the ternary-cluster integral, β_3, among middle segments. If we ignore the higher term of the order of M^{-2}, we may express the chain-end term as[12]

$$A_{3,\beta_3}^{(E)} = a_{3,1}M^{-1} \tag{20}$$

Here, $a_{3,1}$ is given by

$$a_{3,1} = 2N_A^2\beta_{3,1}/M_0^2 \tag{21}$$

with

$$\beta_{3,1} = (\beta_{001}+\beta_{002})/2 \tag{22}$$

β_{00i} denotes the *excess* ternary-cluster integrals among two middle segments (denoted by 0) and one end segment i (i=1,2) over that among three middle segments β_3.

The dotted and dot-dashed lines in Figure 4 show $A_{3,\beta_2}^{(HW)}$ and $A_{3,\beta_2}^{(HW)}+A_{3,\beta_3}^{(0)}$, respectively, according to the above equations, with the parameter set for PS in toluene given in the previous section. Here, we take $\beta_3=4.7\times10^{-3}$ nm^6, which was obtained from the value of A_3 of sufficiently high-molecular-weight PS in cyclohexane at the theta point.[24] Both lines cannot explain the experimental data for $M_w\lesssim10^5$. By adding $A_{3,\beta_3}^{(E)}$ with $a_{3,1}$=8 cm^6 g^{-2} to the dot-dashed line, we obtain the solid line, which is somewhat closer to the data points. However, the agreement is limited to a restricted molecular weight range.

A better fit can be obtained if we use $\beta_3=1.8\times10^{-2}$ nm^6, a much larger β_3 than the one used above, as shown by the dot-dashed line in Figure 5 for $A_{3,\beta_2}^{(HW)}+A_{3,\beta_3}^{(0)}$. Use of such a large β_3 was suggested by Koyama and Sato.[19] The solid and dashed lines in Figure 5 were obtained by adding $A_{3,\beta_3}^{(E)}$ with $a_{3,1}$=1.0 and 3.0 cm^6 g^{-2}, respectively, to the dot-dashed line. This led to satisfactory fits to the data points for benzyl- and butyl-PS, respectively. From these values of $a_{3,1}$, we calculate $\beta_{3,1}$ to be 0.015 and 0.045 nm^6

for the benzyl- and butyl-PS, respectively. The former $\beta_{3,1}$ gives β_{001}=0.015 nm^6 for the benzyl end. The latter, with this β_{001}, gives β_{002}=0.075 nm^6 for the butyl end. These results show that β_{002} is about five times larger than β_{001}.

The β_3 value used for Figure 5 suggests that β_3 in toluene at 15 °C is about four times larger than that in cyclohexane at 34.5°C. This seems rather odd because calculations on rigid spheres with the Lennard–Jones potential show that β_3 at the Boyle point (corresponding to the theta point) is larger than the one at higher temperatures.[25] Furthermore, if we calculate β_3/β_2^2 from the above β_3 and β_2=0.041 nm^3, as estimated from λB=0.33, we obtain β_3/β_2^2=11, which is much larger than the rigid-sphere value of 0.625. However, the β_3 term of Equation (19) only adds a constant to A_3. It is likely that we overlooked a contribution independent of molecular weight, although we do not know what it is.

CONCLUSION

By combining the data for A_2 and A_3 for low-molecular-weight butyl- and benzyl-PS, we estimated the excess binary-cluster integrals (β_{01} and β_{02}) between chain-end and middle segments, as well as the excess ternary-cluster integrals (β_{001} and β_{002}) among one chain-end segment and two middle segments. The conclusions obtained from the study are summarized as follows: (1) β_{02} for the interaction between the butyl end and middle segments is about three times larger than β_{01} for the interaction between the benzyl end and middle segments. (2) The data analysis of A_3 suggested a contribution that is independent of molecular weight by some effect. (3) If we assume such a contribution, β_{002} for the interaction among one butyl end and two middle segments is estimated to be about five times larger than β_{001} for the interaction among one benzyl end and two middle segments.

ACKNOWLEDGEMENTS

We thank Professor Takenao Yoshizaki of Kyoto University for valuable discussions.

1 Yamakawa, H. *Modern Theory of Polymer Solutions* (Harper & Row, New York, 1971).
2 Fujita, H. *Polymer Solutions* (Elsevier, Amsterdam, 1990).
3 Yamakawa, H. *Helical Wormlike Chains in Polymer Solutions* (Springer, Berlin, 1997).
4 Yamakawa, H. On the theory of the second virial coefficient for polymer chains. *Macromolecules* **25,** 1912–1916 (1992).
5 Einaga, Y., Abe, F. & Yamakawa, H. Second virial coefficients of oligo- and polystyrenes. Effects of chain ends. *Macromolecules* **26,** 6243–6250 (1993).
6 Mizuno, T., Terao, K., Nakamura, Y. & Norisuye, T. Second and third virial coefficients of polystyrene with benzyl ends near the Θ point. *Macromolecules* **38,** 4432–4437 (2005).
7 Sato, T., Norisuye, T. & Fujita, H. Second and third virial coefficients for binary polystyrene mixtures in benzene. *J. Polym. Sci. Part B: Polym. Phys.* **25,** 1–17 (1987).
8 Bawn, C. E. H., Freeman, R. F. J. & Kamaliddin, A. R. High polymer solutions part II. The osmotic pressures of polystyrene solutions. *Trans. Faraday Soc.* **46,** 862–872 (1950).
9 Nakamura, Y., Norisuye, T. & Teramoto, A. Third virial coefficient of polystyrene in benzene. *J. Polym. Sci. Part B: Polym. Phys.* **29,** 153–159 (1991).
10 Norisuye, T., Nakamura, Y. & Akasaka, K. Reduced third virial coefficient for linear flexible polymers in good solvents. *Macromolecules* **26,** 3791–3794 (1993).
11 Osa, M., Yoshizaki, T. & Yamakawa, H. Some comments on the analysis of the third virial coefficient for polymer chains. *Polym. J.* **36,** 634–641 (2004).
12 Yamakawa, H., Abe, F. & Einaga, Y. Effects of chain ends on the third virial coefficient for polymer chains. Oligo- and polystyrenes and oligo- and poly(methyl methacrylate)s. *Macromolecules* **27,** 3272–3275 (1994).
13 Tsukahara, Y., Inoue, J., Ohta, Y., Kohjiya, S. & Okamoto, Y. Preparation and characterization of α-benzyl-ω-vinylbenzyl polystyrene macromonomer. *Polym. J.* **26,** 1013–1018 (1994).
14 Lechner, M. D. & Steinmeier, D. G. *Polymer Handbook, 3rd Ed.* (eds. Brandrup, J. & Immergut, E. H.), Ch. VII, 61–148 (Wiley Interscience, 1989).
15 Rubingh, D. N. & Yu, H. Characterization of stiff chain macromolecules. Poly(*n*-hexyl isocyanate) in *n*-hexane. *Macromolecules* **9,** 681–685 (1976).
16 Berry, G. C. Thermodynamic and conformational properties of polystyrene. I. Light-scattering studies on dilute solutions of linear polystyrenes. *J. Chem. Phys.* **44,** 4550–4564 (1966).
17 Barrett, A. J. Second osmotic virial coefficient for linear excluded volume polymer solutions. *Macromolecules* **18,** 196–200 (1985).
18 Abe, F., Einaga, Y., Yoshizaki, T. & Yamakawa, H. Excluded-volume effects on the mean-square radius of gyration of oligo- and polystyrenes in dilute solutions. *Macromolecules* **26,** 1884–1890 (1993).
19 Koyama, R. & Sato, T. Thermodynamic properties of toluene solutions of low molecular weight polystyrenes over wide ranges of concentration. *Macromolecules* **35,** 2235–2242 (2002).
20 Norisuye, T. & Nakamura, Y. Effects of three-segment interactions on the temperature dependence of the third viral coefficient for flexible chains near the Θ point. *Macromolecules* **27,** 2054–2057 (1994).
21 Domb, C. & Barrett, A. J. Universality approach to the expansion factor of a polymer chain. *Polymer* **17,** 179–184 (1976).
22 Shimada, J. & Yamakawa, H. Statistical mechanics of helical worm-like chains. XV. Excluded-volume effects. *J. Chem. Phys.* **85,** 591–600 (1986).
23 Zimm, B. H. Application of the methods of molecular distribution to solutions of large molecules. *J. Chem. Phys.* **14,** 164–179 (1946).
24 Nakamura, Y., Norisuye, T. & Teramoto, A. Second and third virial coefficients for polystyrene in cyclohexane near the Θ point. *Macromolecules* **24,** 4904–4908 (1991).
25 Barker, J. A., Leonard, P. J. & Pompe, A. Fifth virial coefficients. *J. Chem. Phys.* **44,** 4206–4211 (1966).